Probing individual-level structural atrophy in frontal glioma patients

Guobin Zhang[1#], Huawei Huang[2#], Xiaokang Zhang[1#], Yonggang Wang[1], Haoyi Li[1], Yunyun Duan[3], Hongyan Chen[3], Yaou Liu[3], Bin Jing[4*], Song Lin[1*]

[1]Department of Neurosurgery, China National Clinical Research Center for Neurological Diseases (NCRC-ND), Center of Brain Tumor, Beijing Institute for Brain Disorders, Beijing Key Laboratory of Brian Tumor, Beijing Tiantan Hospital, Capital Medical University, Beijing, 100070, China

[2]Department of Critical Care Medicine, Beijing Tiantan Hospital, Capital Medical University, Beijing, 100070, China

[3]Department of Radiology, Beijing Tiantan Hospital, Capital Medical University, Beijing, 100070, China

[4]School of Biomedical Engineering, Capital Medical University, Beijing,100069, China

[#]Guobin Zhang, Huawei Huang and Xiaokang Zhang contributed equally and should be considered joint first author.

[*]Bin Jing and Song Lin should be considered joint senior author.

***Corresponding author**

Name: Song Lin

Affiliation: Department of Neurosurgery, China National Clinical Research Center for Neurological Diseases (NCRC-ND), Center of Brain Tumor, Beijing Institute for Brain Disorders, Beijing Key Laboratory of Brain Tumor, Beijing Tiantan Hospital, Capital Medical University

Address: South 4th Ring West Road 119, Fengtai District, Beijing, 100070, China

E-mail: linsong_ttyy@sina.com

Tel: +86 010 59976509

Fax: +86 010 59976509

Name: Bin Jing

Affiliation: School of Biomedical Engineering, Capital Medical University

Address: No.10 Xi Tou Tiao, You'an Men Wai, Fengtai District, Beijing, 100069, China

E-mail: bjing@ccmu.edu.cn

Tel: (+86) 15011101291

Fax: +86 010 83911552

Data Availability: The data that support the findings of this study are available from the corresponding author upon reasonable request.

Funding: This work was supported by the National Natural Science Foundation of China (81801042), Beijing Hospital Authority Youth Programme (20190504), Beijing Outstanding Talent Training Foundation, Youth Backbone Individual Project (2018000021469G230) and Beijing Municipal Commission of Education (KM202010025025). The funds had no role in the study design, data collection and analysis, decision to publish, or manuscript preparation.

Conflict of Interest: The authors declare that they have no competing interests.

Ethics approval: The study was approved by the Institutional Review Board of Beijing Tiantan Hospital, Capital Medical University, Beijing, China (KY2020-048-01).

Patient consent: Written informed consent was obtained from all patients.

Acknowledgments: None.

Abstract

Although every glioma patient varies in tumor size, location, histological grade and molecular biomarkers, structural abnormalities are commonly conducted in a group-level, leading to the miss of individual structural atrophy. In this study, we introduced an individual-level structural abnormality detection method for glioma patients and proposed several novel abnormality indexes to depict the individual atrophy pattern. Forty-five glioma patients in frontal lobe and fifty-two age-matched healthy controls participated in the study. All patients underwent neurocognitive test and molecular examinations, including 1p/19q co-deletion, isocitrate dehydrogenase (IDH) mutation, telomerase reverse transcriptase (TERT) promoter mutation and O6-methylguanine-DNA methyltransferase (MGMT) promotor methylation. Individual structural abnormality maps for every glioma patient were calculated from the preoperative T1 images, and the individual abnormality index were further computed and explored the associations with clinical indicators. The results manifested that: 1. Every glioma patient show unique atrophy pattern; 2. Glioma patients also share consistent atrophy regions; 3. The atrophy pattern is influenced by some molecular biomarkers. Our study provides an effective way to access the individual structural abnormalities in glioma patients, and displays great potentials in individualized precision medicine for glioma patients.

Keywords: frontal glioma, structural MRI, individual structural atrophy, abnormality index, molecular indicators

Introduction

Gliomas represent the majority of primary central nervous system (CNS) malignant tumors, and the surgical outcomes are dependent on the comprehensive acquirement of various diagnostic information including histological grades and molecular biomarkers. However, these golden standard indicators are hard to acquire before neurosurgery, and neuroimaging has consequently served as a key way to perceive the glioma status. There are many imaging modalities collected for glioma patients, such as diffusion weighted/tensor imaging (DWI/DTI), resting-state functional MRI (rs-fMRI), positron emission tomography (PET) and structural magnetic resonance imaging (sMRI). Among them, sMRI (e.g. T1, T2) is an easy-to-collect and economical modality with high spatial resolution and test-retest reliability, which is thus widely collected in most neurosurgical centers. Usually, neurosurgeons only take qualitative evaluations for the tumor regions on structural images through visual inspection, and an individual-level quantitative analysis for tumor-related alterations is still lacking in clinical presurgical evaluation.

With the appearance of Radiomics, the quantitative analysis for the tumor region on structural images has been demonstrated to provide useful information about the histological/molecular biomarkers(Lohmann et al., 2018; Lu et al., 2018; Soike et al., 2018; Takahashi et al., 2019). However, the alterations in non-tumor regions are rarely to access in Radiomics studies, which may be also important to the postsurgical prognosis. Although the conventional morphological analysis such as voxel-based

morphometry could detect structural changes (e.g. contralateral hemisphere) for glioma patients, the results are based on the group-level statistical analysis and the structural changes at individual level are still not clear. Specifically, every glioma patient may suffer unique structural alterations in non-tumor regions, and detecting and quantifying individual-level structural alterations may further deepen the understanding of the influences of tumor regions.

In recent years, individualized neuroimaging has appeared and displayed great potentials in precision diagnosis and treatment(Liu, Liu, Wang, & Dahmani, 2020; Wang et al., 2015). Stoecklein et al. found individual functional connectivity characteristics of glioma patients were significantly related with WHO tumor grade and the IDH mutation status(Stoecklein et al., 2020). However, rs-fMRI is not a clinical routine scan sequence, and to collect a high quality rs-fMRI dataset is also challenging for glioma patients. In this condition, sMRI becomes an alternative choice to model the individual alterations in the brain. Previous studies(Perry et al., 2017) have manifested W-score could successfully measure individual gray matter changes in neurological diseases, which is firstly introduced into glioma patients in the study. Furthermore, we extend the W-score method to both gray matter and white matter, and propose several novel structural abnormality indexes to depict the individual structural alteration patterns. The main purposes of the study are to ascertain: 1. Whether frontal glioma patients display unique structural alterations for every subject? 2. Whether frontal glioma patients display consensus structural alterations and where

are they located? 3. Whether individual atrophy patterns vary with clinical and molecular indicators?

Materials and Methods

Patients

The study was approved by the Institutional Review Board of Beijing Tiantan Hospital, Capital Medical University, Beijing, China (KY2020-048-01). The study was also registered at Chinese ClinicalTrial Registry (ChiCTR2000031805). All study procedures were in accordance with the Declaration of Helsinki. Written informed consent was obtained from all patients. Fifty-two glioma patients and one hundred seventeen healthy controls participated this study, which were listed in Table 1. All gliomas in the cohort were diagnosed according to the criteria of the WHO classification system in the revised version of 2016. Inclusion criteria were suspected, newly diagnosed glioma with only one cancer region in the brain and age over 18 years. Exclusion criteria were previous cranial surgery, neuropsychiatric comorbidities, and any contraindications to MR scanning such as metal implants. Neuropsychological testing was conducted prior to the first MRI scan using the *Montreal Cognitive Assessment* (MOCA) test. Histological confirmation of the diagnosis was obtained by surgical resection. Molecular markers, including 1p/19q codeletion, IDH1/2 mutation, TERT promoter mutation and O^6-methylguanine-DNA methyltransferase (MGMT) promotor methylation were all collected. Chromosomes 1 and 19 were analyzed by the fluorescence in situ hybridization method, and the

IDH1/2 mutation and TERT promoter mutation were detected by sequence analysis, both following a previously described protocol(Suh, Kim, Jung, Choi, & Kim, 2019). MGMT promoter methylation was assessed by methylation-specific PCR as described previously by our team(Zhang et al., 2013). Patients were followed with routine clinical visits after initiation of therapy. All age-matched healthy controls were recruited from the local community and university students.

Structural MRI acquirement

All subjects were scanned with a Philips Ingenia 3.0T MRI scanner at Beijing Tiantan Hospital. For both glioma patients and healthy controls, T1 sequence was collected with the following parameters: TR: 6.5 ms, TE: 3.0 ms, Flip angle: 8°, voxel size: $1\times1\times1$ mm^3, image dimension: 256×256×196. In addition, T2-flair was also scanned for glioma patients with the listed parameters: TR: 4.8 s, TE: 0.34 s, Flip angle: 90°, voxel size: $0.625\times0.625\times0.55$ mm^3, image dimension: 400×400×300.

Image processing

The tumor region of every patient was extracted from T2-flair images with two sequential steps: 1. launch an automatic segmentation by ITK-SNAP software; 2. manually correct the segmentation by experienced neurosurgeons. After the segmentation, individual T2-flair image was co-registered to its corresponding T1 image by SPM software, and the transformation matrix was used on the segmented tumor to obtain the matched tumor region in T1 image space.

Individual T1 images were processed with CAT12 software to calculate the brain tissue volume. The skull stripping and correction for bias-field inhomogeneities were subsequently conducted. After that, the whole brain was segmented into different tissue types, e.g. gray matter and white matter. Then, the segmented GM and WM images were normalized to the MNI standard space with a modulation manner by DARTEL algorithm. Finally, the normalized GM and WM images were smoothed with 4-mm FWHM Gaussian kernel.

Individual structural atrophy map

Figure 1 illustrated the flowchart to generate individual structural atrophy map. First of all, all healthy controls were used to construct the normative brain volume model. In this model, general linear model (GLM) was adopted to discover the relationship between voxel-wise volume and variables including age, sex, and total intracranial volume (TIV) as the following equation.

$$volume = \beta_1 \times age + \beta_2 \times sex + \beta_3 \times TIV + residual \qquad (1)$$

Here, β_1, β_2, β_3 were weights for age, sex and TIV on the voxel-wise volume, and GM and WM volume models were respectively constructed.

Once the models had been created, the individual structural abnormality map for each glioma patient was calculated based on W score, which was calculated as following:

$$W\ score = \frac{volume_{patient} - \beta_1 \times age_{patient} - \beta_2 \times sex_{patient} - \beta_3 \times TIV_{patient}}{standard\ deviation\ of\ residuals\ in\ normative\ model} \qquad (2)$$

After the calculation of W score for each patient, a cutoff threshold (|W|>6) and a cluster size (K>100) were set to generate the individual structural abnormality map. Notably, an individualized explicit non-tumor mask was produced for every patient in which individual tumor mask was deleted from the tissue (GM/WM) prior probability template (threshold: 0.2). Based on the individual structural abnormality map, we further proposed 4 novel abnormality indexes on GM/WM to reflect the characteristics of structural damages induced by glioma: Ipsilateral atrophy ratio, Contralateral atrophy ratio, Non-cancer atrophy ratio, Relative atrophy ratio, which were listed in details in Table 2.

Associations with various glioma indicators

To explore the associations between each of 8 abnormality indexes and various glioma indicators, for continuous variables like tumor volume, MGMT methylation, and MOCA score, Spearman correlation was used to ascertain the linear relationship with these atrophy indexes; for categorical variables such as TERT mutation, 1p/19q deletion, histological grade and IDH1, two-sample T test was used to determine whether the atrophy indexes varied with these indicators. An FDR corrected $P < 0.05$ was thought as the significance level for both analyses.

Results

The clinical characteristics for glioma patients

There were 45 glioma patients (mean age 43.2±9.7 years, 29 male) and 51 healthy controls (mean age 42.6±9.7 years, 24 male) that participated in the study. All patients were prospectively included between May 2019 and July 2020. The WHO histological grade, IDH1, TERT mutation, 1p/19q deletion, MGMT methylation were acquired for every patient, and Montreal Cognitive Assessment (MOCA) score was also recorded. Table 1 summarized the demographic and clinical information for all subjects.

Every glioma patient displayed distinct atrophy pattern

All patients only displayed atrophies in GM and WM. Figure 2 illustrated three selected patients' T1 images and corresponding individualized GM/WM atrophy maps (mapping back into T1 space). Obviously, the structural atrophies not only lay in regions close to tumors but also in regions far away from tumors. Although the patients vary in tumor sizes and tumor grades, it is clear that every subject displayed unique atrophy pattern.

Every glioma patient also showed common atrophy regions

Figure 3 displayed the overlapping GM regions in individual structural atrophy map. No matter the tumor is located at the left hemisphere or right hemisphere, the atrophies in right temporal lobe are more obvious than the left one, mainly including hippocampus, amygdala, parahippocampus and thalamus. Moreover, the contralateral frontal regions also displayed some degree of atrophy. Figure 4 exemplified the

consistent WM regions in individual structural atrophy map. The main atrophy regions are located at bilateral thalamus and pallidum, and the contralateral part is more severely atrophied than the ipsilateral part.

Individual brain atrophy indexes were associated with some clinical indicators

Fig 5 illustrated all possible relations between the proposed individual abnormality indexes and clinical indicators, and all of them had passed an FDR correction with $P<0.05$. GM/WM relative atrophy ratio were found to significantly correlate with the tumor size, however, with the increasement of the tumor volume, the relative atrophy ratio was decreased (power law distribution), and no other individual structural indexes were related with tumor size. WM contralateral atrophy ratio was found with significant differences between IDH wild type and mutation type, while WM relative atrophy ratio were obviously different between 1p/19q wild type and mutation type. Moreover, both GM/WM relative atrophy ratio displayed between-group differences in TERT wild type and mutation type. No other relationships were detected with MOCA and MGMT.

Discussion

In this study, we firstly depicted individual non-tumor structural atrophy characteristics for glioma patients, and proposed several quantitative indexes to ascertain the relationship between individual atrophy patterns and clinical indicators. The results demonstrated every glioma patient displays distinct atrophy pattern but

also shared overlapping atrophy regions. In addition, several atrophy indexes were related with tumor size and molecular indicators.

Neuroimaging has acted as indispensable tool for presurgical assessment of glioma patients. However, most imaging studies only focus on the tumor region in order to judge the status of tumor, and the non-tumor alterations are rarely to access. Moreover, neuroimaging is usually used by two conventional manner: 1. visual inspection by experienced neurosurgeons; 2. group-level statistical comparison between glioma patients and healthy controls. Both manners may miss the individual unique changes in non-tumor regions. Our study firstly offers an individual-level manner to describe individual atrophy in every glioma patient, and manifested that every glioma patient displays unique structural atrophy in non-tumor regions, which was consistent with previous individual fMRI study(Stoecklein et al., 2020). Taken together, glioma may lead to patient-specific alterations in both brain function and structure, and individualized neuroimaging methods show great potentials in the pre-surgical evaluation and post-surgical prognosis estimation.

Although glioma patients display distinct structural atrophy at the individual level, it is interesting to find they also share overlapping GM atrophies in regions like bilateral hippocampus, amygdala, thalamus and parahippocampus. Specially, these atrophies are not dependent on the hemisphere of tumor, tumor size, histological grade or molecular indicators, indicating that frontal glioma could introduce systematic

atrophy in brain structure. In addition, GM atrophy were more obvious in right temporal lobe than the left one regardless the tumor hemisphere, implying right temporal lobe is more vulnerable to the frontal tumor, and there is lateralization in the structural damages induced by the frontal tumor. Previous literatures have reported that as many as 90% of brain tumor patients would show tumor-related cognitive deficits (e.g., memory, attention, information processing, executive function)(Gehring, Roukema, & Sitskoorn, 2012; Gehring, Sitskoorn, Aaronson, & Taphoorn, 2008), which may be explained by the current findings that limbic system including hippocampus, amygdala, parahippocampus and thalamus are damaged in glioma patients.

The consistent WM atrophies were mainly located at bilateral thalamus and pallidum, and the contralateral hemisphere was more severely atrophied than the ipsilateral one. These regions are involved in two fiber bundles linking fronto-temporal regions: superior longitudinal fasciculus (SLF) and uncinate fasciculus (UF). SLF has been reported to correlate with the spatial working memory deficit(Kinoshita et al., 2016), visuospatial dysfunction(Nakajima et al., 2017) and transmission of speech and language(Henderson, Abdullah, Verma, & Brem, 2020) in glioma patients. UF has been demonstrated to relate with the language(Duffau, Gatignol, Moritz-Gasser, & Mandonnet, 2009) and cognitive deficits(Incekara, Satoer, Visch-Brink, Vincent, & Smits, 2018) in glioma patients. The common WM atrophies also prompt the possible cognitive damages in frontal glioma patients, and may provide a possible pathway

283 that link the remote GM atrophy covariation.

284

285 GM/WM relative atrophy ratio but not other individual indexes were negatively
286 related (in fact power law distribution) with tumor volume, and two conclusions may
287 thereby be generated: 1. the volume of atrophy in the brain was in fact not dependent
288 on the tumor volume; 2. the relative atrophy volume becomes smaller when the tumor
289 volume enlarges. Moreover, WM contralateral/relative atrophy ratio were found with
290 significant differences in IDH and 1p/19q mutation. IDH and 1p/19q are both known
291 indicators for the prognosis of glioma patients. For example, lower grade gliomas
292 with wild-type IDH were reported to show similar prognosis with glioblastomas, and
293 IDH mutated glioblastomas were found with better prognosis than IDH wild-type
294 glioblastomas(Darvishi et al., 2020; Hartmann et al., 2010). In addition, anaplastic
295 gliomas with IDH wild-type have worse prognosis than glioblastomas with IDH
296 mutation(Hartmann et al., 2010). 1p/19q co-deletion is found with better prognosis for
297 patients with oligodendroglioma after radiotherapy or alkylating
298 chemotherapy(Jenkins et al., 2006; van der Voort et al., 2019). Additionally, GM/WM
299 relative atrophy ratio were found differences in TERT mutation, which is also a
300 promising indicator for the treatment response of radiotherapy and temozolomide in
301 primary glioblastoma multiforme (GBM)(Eckel-Passow et al., 2015; Peng et al., 2020;
302 Vuong et al., 2017; Yang et al., 2016; Yuan et al., 2016). In summary, individual
303 structural atrophy patterns are influenced by the genetic type.

304

Finally, several limitations should be mentioned: 1. The optimal threshold for W is not clear, and we chose |W|>6 in order to reduce the false positive rate in atrophy detection. 2. The gender and TIV are not well matched between glioma patients and healthy controls, and future studies could involve more patients from multicenter to verify the robustness of the current findings.

Conclusion

Our study firstly depicted the individual atrophy pattern for glioma patients, and found individual structural atrophy was unique and driven by genetic information. Our findings could provide valuable information for the individualized presurgical evaluation and postsurgical prognosis.

Reference

Darvishi, P., Batchala, P. P., Patrie, J. T., Poisson, L. M., Lopes, M. B., Jain, R., . . . Patel, S. H. (2020). Prognostic Value of Preoperative MRI Metrics for Diffuse Lower-Grade Glioma Molecular Subtypes. *AJNR Am J Neuroradiol, 41*(5), 815-821. doi:10.3174/ajnr.A6511

Duffau, H., Gatignol, P., Moritz-Gasser, S., & Mandonnet, E. (2009). Is the left uncinate fasciculus essential for language? A cerebral stimulation study. *J Neurol, 256*(3), 382-389. doi:10.1007/s00415-009-0053-9

Eckel-Passow, J. E., Lachance, D. H., Molinaro, A. M., Walsh, K. M., Decker, P. A., Sicotte, H., . . . Jenkins, R. B. (2015). Glioma Groups Based on 1p/19q, IDH, and TERT Promoter Mutations in Tumors. *N Engl J Med, 372*(26), 2499-2508. doi:10.1056/NEJMoa1407279

Gehring, K., Roukema, J. A., & Sitskoorn, M. M. (2012). Review of recent studies on interventions for cognitive deficits in patients with cancer. *Expert Rev Anticancer Ther, 12*(2), 255-269. doi:10.1586/era.11.202

Gehring, K., Sitskoorn, M. M., Aaronson, N. K., & Taphoorn, M. J. (2008). Interventions for cognitive deficits in adults with brain tumours. *Lancet Neurol, 7*(6), 548-560. doi:10.1016/s1474-4422(08)70111-x

Hartmann, C., Hentschel, B., Wick, W., Capper, D., Felsberg, J., Simon, M., . . . von Deimling, A. (2010). Patients with IDH1 wild type anaplastic astrocytomas exhibit worse prognosis than IDH1-mutated glioblastomas, and IDH1 mutation status accounts for the unfavorable prognostic effect of higher age: implications for classification of gliomas. *Acta Neuropathol, 120*(6), 707-718. doi:10.1007/s00401-010-0781-z

Henderson, F., Abdullah, K. G., Verma, R., & Brem, S. (2020). Tractography and the connectome in neurosurgical treatment of gliomas: the premise, the progress, and the potential. *Neurosurg Focus, 48*(2), E6. doi:10.3171/2019.11.Focus19785

Incekara, F., Satoer, D., Visch-Brink, E., Vincent, A., & Smits, M. (2018). Changes in language white matter tract microarchitecture associated with cognitive deficits in patients with presumed low-grade glioma. *J Neurosurg*, 1-9. doi:10.3171/2017.12.Jns171681

Jenkins, R. B., Blair, H., Ballman, K. V., Giannini, C., Arusell, R. M., Law, M., . . . Buckner, J. C. (2006). A t(1;19)(q10;p10) mediates the combined deletions of 1p and 19q and predicts a better prognosis of patients with oligodendroglioma. *Cancer Res, 66*(20), 9852-9861. doi:10.1158/0008-5472.Can-06-1796

Kinoshita, M., Nakajima, R., Shinohara, H., Miyashita, K., Tanaka, S., Okita, H., . . . Hayashi, Y. (2016). Chronic spatial working memory deficit associated with the superior longitudinal fasciculus: a study using voxel-based lesion-symptom mapping and intraoperative direct stimulation in right prefrontal glioma surgery. *J Neurosurg, 125*(4), 1024-1032. doi:10.3171/2015.10.Jns1591

Liu, H., Liu, W. J., Wang, D., & Dahmani, L. (2020). Individual-Specific Analysis for Psychoradiology. *Neuroimaging Clin N Am, 30*(1), 45-51. doi:10.1016/j.nic.2019.09.003

Lohmann, P., Lerche, C., Bauer, E. K., Steger, J., Stoffels, G., Blau, T., . . . Galldiks, N. (2018). Predicting IDH genotype in gliomas using FET PET radiomics. *Sci Rep, 8*(1), 13328. doi:10.1038/s41598-018-31806-7

Lu, C. F., Hsu, F. T., Hsieh, K. L., Kao, Y. J., Cheng, S. J., Hsu, J. B., . . . Chen, C. Y. (2018). Machine Learning-Based Radiomics for Molecular Subtyping of Gliomas. *Clin Cancer Res, 24*(18),

4429-4436. doi:10.1158/1078-0432.Ccr-17-3445

Nakajima, R., Kinoshita, M., Miyashita, K., Okita, H., Genda, R., Yahata, T., . . . Nakada, M. (2017). Damage of the right dorsal superior longitudinal fascicle by awake surgery for glioma causes persistent visuospatial dysfunction. *Sci Rep, 7*(1), 17158. doi:10.1038/s41598-017-17461-4

Peng, H., Huo, J., Li, B., Cui, Y., Zhang, H., Zhang, L., & Ma, L. (2020). Predicting Isocitrate Dehydrogenase (IDH) Mutation Status in Gliomas Using Multiparameter MRI Radiomics Features. *J Magn Reson Imaging*. doi:10.1002/jmri.27434

Perry, D. C., Brown, J. A., Possin, K. L., Datta, S., Trujillo, A., Radke, A., . . . Seeley, W. W. (2017). Clinicopathological correlations in behavioural variant frontotemporal dementia. *Brain, 140*(12), 3329-3345. doi:10.1093/brain/awx254

Soike, M. H., McTyre, E. R., Shah, N., Puchalski, R. B., Holmes, J. A., Paulsson, A. K., . . . Chan, M. D. (2018). Glioblastoma radiomics: can genomic and molecular characteristics correlate with imaging response patterns? *Neuroradiology, 60*(10), 1043-1051. doi:10.1007/s00234-018-2060-y

Stoecklein, V. M., Stoecklein, S., Galiè, F., Ren, J., Schmutzer, M., Unterrainer, M., . . . Liu, H. (2020). Resting-state fMRI detects alterations in whole brain connectivity related to tumor biology in glioma patients. *Neuro Oncol, 22*(9), 1388-1398. doi:10.1093/neuonc/noaa044

Suh, C. H., Kim, H. S., Jung, S. C., Choi, C. G., & Kim, S. J. (2019). Imaging prediction of isocitrate dehydrogenase (IDH) mutation in patients with glioma: a systemic review and meta-analysis. *Eur Radiol, 29*(2), 745-758. doi:10.1007/s00330-018-5608-7

Takahashi, S., Takahashi, W., Tanaka, S., Haga, A., Nakamoto, T., Suzuki, Y., . . . Saito, N. (2019). Radiomics Analysis for Glioma Malignancy Evaluation Using Diffusion Kurtosis and Tensor Imaging. *Int J Radiat Oncol Biol Phys, 105*(4), 784-791. doi:10.1016/j.ijrobp.2019.07.011

van der Voort, S. R., Incekara, F., Wijnenga, M. M. J., Kapas, G., Gardeniers, M., Schouten, J. W., . . . Smits, M. (2019). Predicting the 1p/19q Codeletion Status of Presumed Low-Grade Glioma with an Externally Validated Machine Learning Algorithm. *Clin Cancer Res, 25*(24), 7455-7462. doi:10.1158/1078-0432.Ccr-19-1127

Vuong, H. G., Altibi, A. M. A., Duong, U. N. P., Ngo, H. T. T., Pham, T. Q., Chan, A. K., . . . Hassell, L. (2017). TERT promoter mutation and its interaction with IDH mutations in glioma: Combined TERT promoter and IDH mutations stratifies lower-grade glioma into distinct survival subgroups-A meta-analysis of aggregate data. *Crit Rev Oncol Hematol, 120*, 1-9. doi:10.1016/j.critrevonc.2017.09.013

Wang, D., Buckner, R. L., Fox, M. D., Holt, D. J., Holmes, A. J., Stoecklein, S., . . . Liu, H. (2015). Parcellating cortical functional networks in individuals. *Nat Neurosci, 18*(12), 1853-1860. doi:10.1038/nn.4164

Yang, P., Cai, J., Yan, W., Zhang, W., Wang, Y., Chen, B., . . . Jiang, T. (2016). Classification based on mutations of TERT promoter and IDH characterizes subtypes in grade II/III gliomas. *Neuro Oncol, 18*(8), 1099-1108. doi:10.1093/neuonc/now021

Yuan, Y., Qi, C., Maling, G., Xiang, W., Yanhui, L., Ruofei, L., . . . Qing, M. (2016). TERT mutation in glioma: Frequency, prognosis and risk. *J Clin Neurosci, 26*, 57-62. doi:10.1016/j.jocn.2015.05.066

Zhang, G. B., Cui, X. L., Sui, D. L., Ren, X. H., Zhang, Z., Wang, Z. C., & Lin, S. (2013). Differential molecular genetic analysis in glioblastoma multiforme of long- and short-term survivors: a clinical study in Chinese patients. *J Neurooncol, 113*(2), 251-258.

 doi:10.1007/s11060-013-1102-x

405 **Table 1** The demographic and clinical information of all subjects.

	Glioma patients	Healthy controls
Number	45	51
Gender (M/F)	29/16	24/27
Age	43.2±9.7	42.6±9.7
TIV	1475.1±114.0	1425.9±144.9
Tumor volume	37.6±38.0	-
Histological grade (□/□/□)	33/10/2	-
IDH1 mutation (mutated/wild)	39/6	-
TERT promoter mutation (mutated/wild)	33/19	-
1p/19q deletion (both 1p/19q /only 19q/only 1p/none)	24/2/4/15	-
MGMT promoter methylation	0.25±0.16	-
MOCA	22.6±4.6	-

406 Abbreviation: IDH, isocitrate dehydrogenase; MGMT, O^6-methylguanine-DNA methyltransferase;
407 MOCA, Montreal Cognitive Assessment; TERT, telomerase reverse transcriptase; TIV, total
408 intracranial volume.
409

410 **Table 2** The proposed 8 structural abnormality indexes.

Abnormality index	Description
Ipsilateral atrophy ratio	$= \frac{number\ of\ GM/WM\ atrophy\ voxels\ in\ hemisphere\ with\ tumor}{number\ of\ all\ voxels\ in\ hemisphere\ with\ tumor}$
Contralateral atrophy ratio	$= \frac{number\ of\ GM/WM\ atrophy\ voxels\ in\ contralateral\ hemisphere}{number\ of\ all\ voxels\ in\ contralateral\ hemisphere}$
Non-cancer atrophy ratio	$= \frac{number\ of\ abnormal\ GM/WM\ voxels\ in\ non-cancer\ region}{number\ of\ all\ voxels\ in\ whole\ brain}$
Relative atrophy ratio	$= \frac{number\ of\ abnormal\ GM/WM\ voxels\ in\ non-cancer\ region}{number\ of\ all\ voxels\ in\ cancer\ region}$

411 Abbreviation: GM, gray matter; WM, white matter.

412 ## Figure legends

413 **Figure 1** The flowchart of the proposed structural abnormality indexes: (A). the construction of

414 normative brain volume model; (B). the calculation of the proposed individual abnormality indexes.

415

416 **Figure 2** Three examples of individualized GM/WM abnormality maps.

417

418 **Figure 3** Overlapping gray matter atrophy in non-tumor regions for all patients with tumor on (A) left

419 hemisphere and (B) right hemisphere.

420

421 **Figure 4** Overlapping white matter atrophy in non-tumor regions for all patients with tumor on left

422 hemisphere and right hemisphere.

423

424 **Figure 5** The relationship between abnormality indexes and clinical/molecular indicators.

425

426

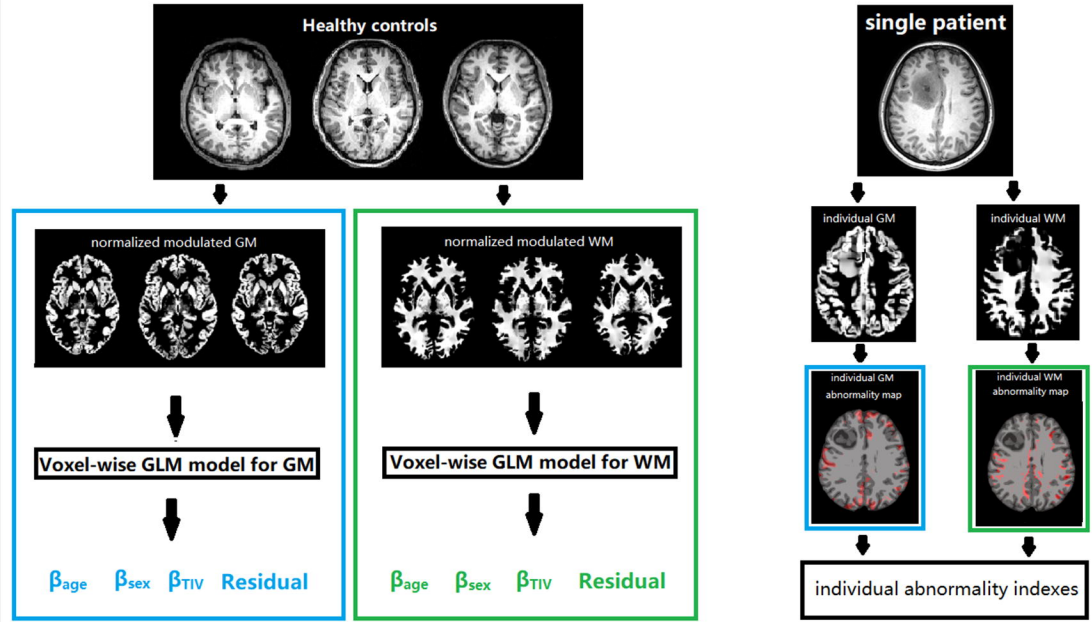
Healthy controls
normalized modulated GM
normalized modulated WM
Voxel-wise GLM model for GM
Voxel-wise GLM model for WM
βage βsex βTIV Residual
βage βsex βTIV Residual
(A)
single patient
individual GM
individual WM
individual GM abnormality map
individual WM abnormality map
individual abnormality indexes
(B)

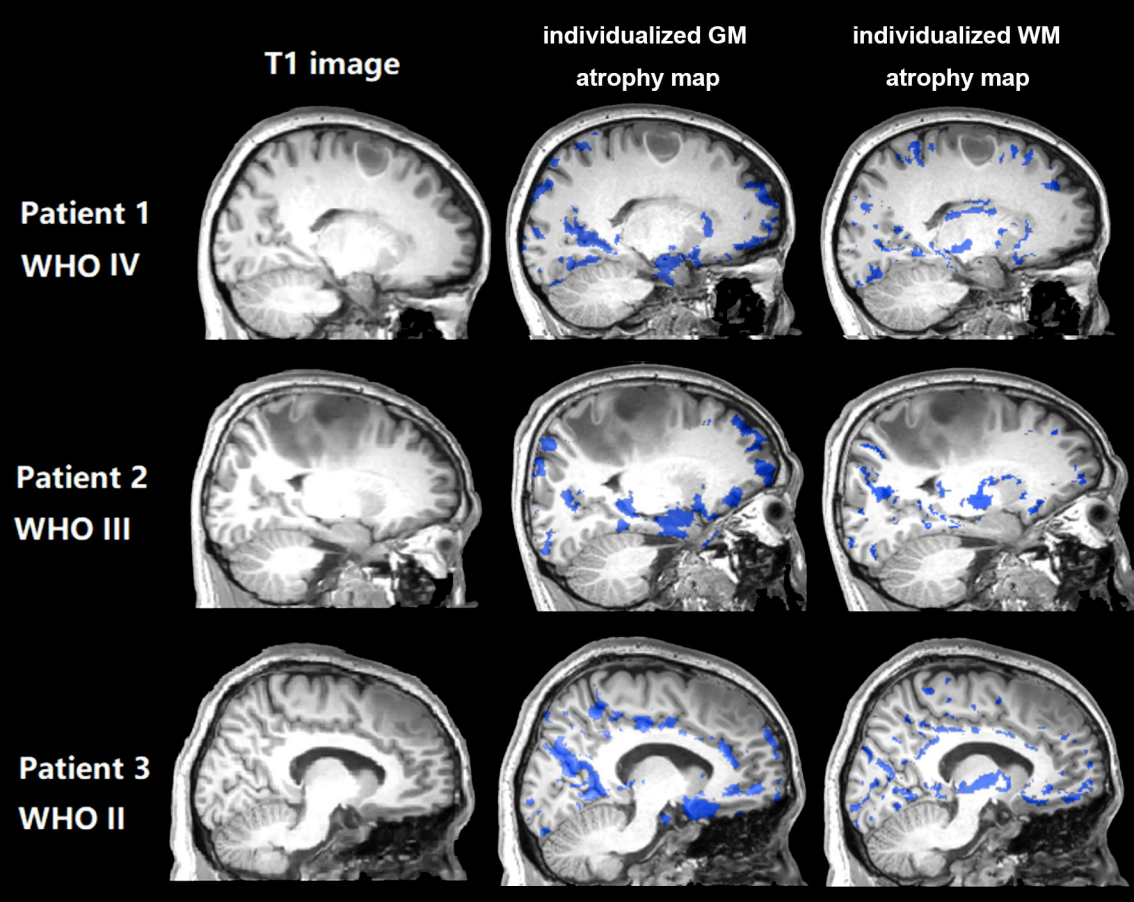
T1 image
individualized GM atrophy map
individualized WM atrophy map
Patient 1
WHO IV
Patient 2
WHO III
Patient 3
WHO II

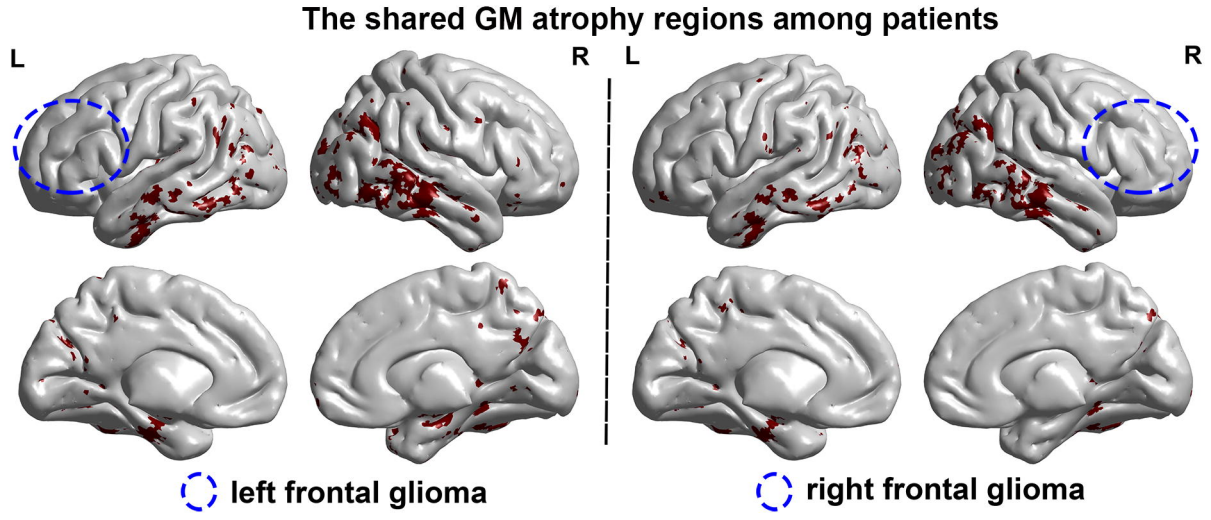
The shared GM atrophy regions among patients
L
R
L
R
left frontal glioma
right frontal glioma

The shared WM atrophy regions among patients

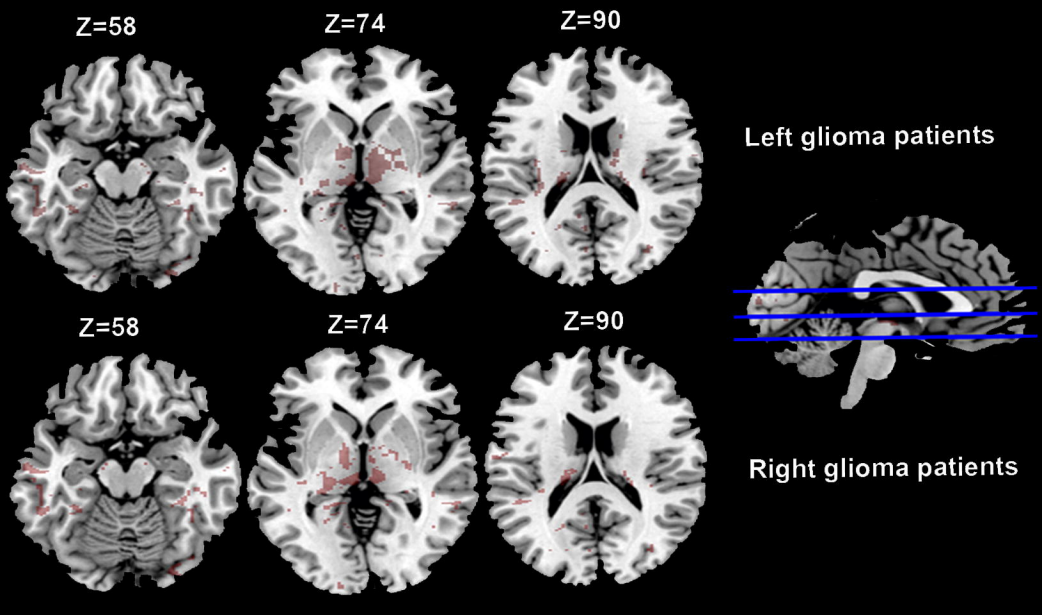

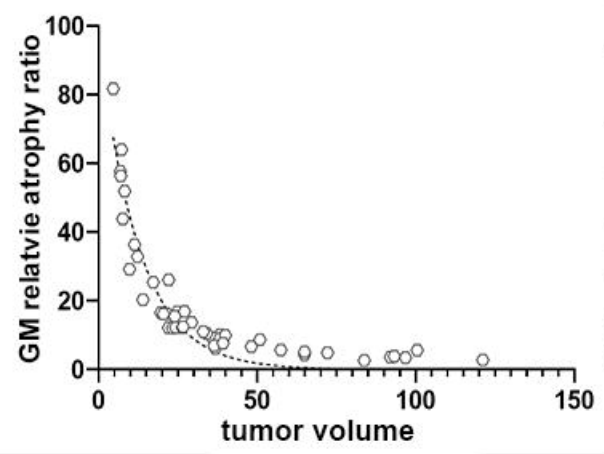
GM relatvie atrophy ratio
100
80
60
40
20
0
0
50
100
150
tumor volume

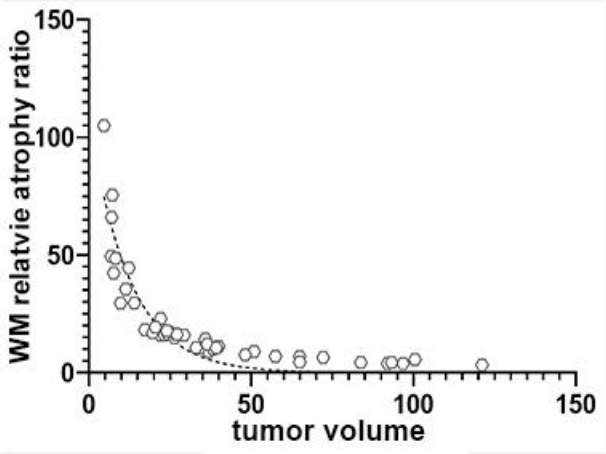
WM relatvie atrophy ratio
150
100
50
0
0
50
100
150
tumor volume

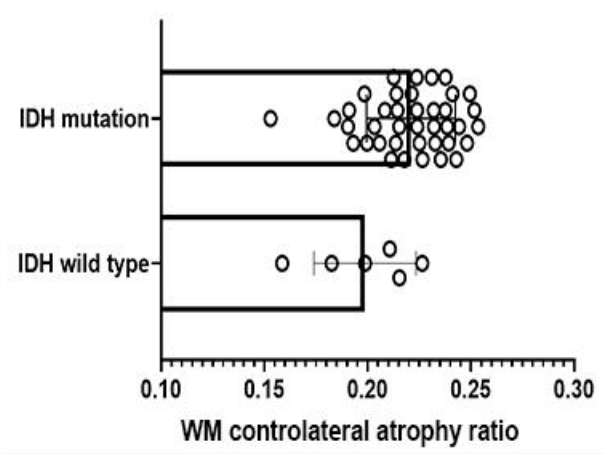
IDH mutation
IDH wild type
0.10
0.15
0.20
0.25
0.30
WM controlateral atrophy ratio

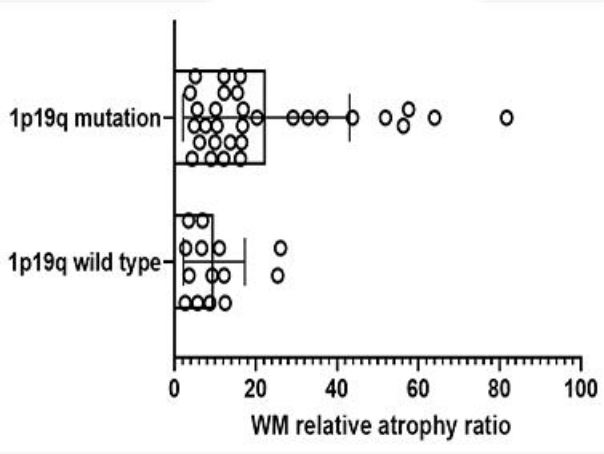
1p19q mutation
1p19q wild type
0
20
40
60
80
100
WM relative atrophy ratio

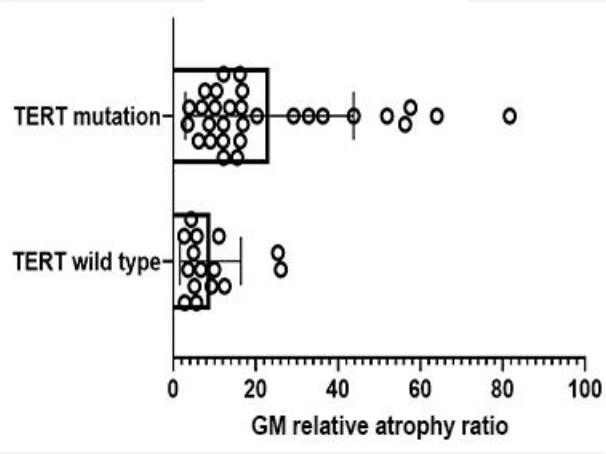
TERT mutation
TERT wild type
0
20
40
60
80
100
GM relative atrophy ratio

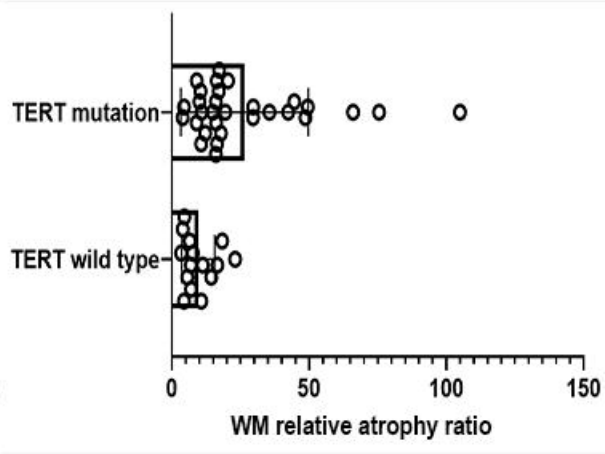
TERT mutation
TERT wild type
0
50
100
150
WM relative atrophy ratio